Nanoscale

RSC Publishing

PAPER

Non-monotonic size change of monodisperse Fe_3O_4 nanoparticles in the scale-up synthesis†

Cite this: *Nanoscale*, 2013, **5**, 2804

Ning-Ning Song,[a] Hai-Tao Yang,*[a] Xiao Ren,[a] Zi-An Li,[b] Yi Luo,[a] Jun Shen,[c] Wen Dai,[c] Xiang-Qun Zhang[a] and Zhao-Hua Cheng*[a]

Received 5th December 2012
Accepted 12th January 2013

DOI: 10.1039/c3nr33950e

www.rsc.org/nanoscale

A non-monotonic size change of monodisperse Fe_3O_4 nanoparticles (NPs) with a diameter of 3–20 nm is observed in the scale-up organic-phase synthesis. The crystal structures and the valence state of the Fe ions of the as-prepared NPs were determined by X-ray diffraction (XRD) and Mössbauer spectroscopy, respectively. It is interestingly observed that particle size does not decrease monotonously with either the increase of the molar ratio of oleic acid (OA) to FeO·OH, or the decrease of precursor concentration. Furthermore, the reaction process was investigated *via* the time-dependent Fourier transform infrared spectra (FTIR) and the transmission electron microscopy (TEM) images, which reveal that the non-monotonic size change results from the different influence of OA on the three reaction stages including monomer formation, nucleation, and growth with increasing precursor amounts.

I Introduction

Magnetic NPs with their capability of being manipulated under a magnetic field provides a controllable means of magnetically tagging biomolecules or cells. These novel properties are of great potential application in highly efficient bioseparation/drug delivery, highly sensitive bio-sensing, magnetic resonance imaging (MRI) contrast enhancement, and magnetic fluid hyperthermia.[1–3] In the family of magnetic NPs, magnetite (Fe_3O_4) has recently attracted much attention due to its high Curie temperature ($T_c \sim 850$ K), good biocompatibility, high magnetic moment, and relatively good air-stability. In order to realize the application in both biomedical and many nano-technology fields, the gram-scale or kilogram-scale synthesis of size-controlled monodisperse Fe_3O_4 NPs with high saturation magnetization is of key importance. Recently, high-temperature organic-phase methods using various precursors such as $Fe(CO)_5$, $Fe(acac)_3$, and $Fe(OA)_3$, have widely been applied since they have the overwhelming advantage of well-controlling the dispersion, crystallization, size, and shape compared to traditional co-precipitation in an aqueous solution. In particular, hydrophobic NPs can be transformed into hydrophilic ones by ligand exchange coupling, allowing the preparation of aqueous NP dispersions for biomedical applications.[4] However, as a laboratory technique, high-temperature organic-phase methods are usually used to prepare several or dozens of micrograms of monodisperse NPs. Until now, only Hyeon's group reported a gram-scale synthesis of iron oxide NPs using the thermal decomposition of iron oleate.[5] Moreover, in the scale-up synthesis, the law for controlling the size and shape does not abide by a simple multiple relationship and would be greatly different from that previously determined at the microgram-scale. Some researchers have observed that a change of the ratio of surfactant/precursor and even the ratio of two combined surfactants has a strong influence on particle size, shape, and size distribution. For example, Yang has observed that the oleic acid (OA)/$Fe(CO)_5$ molar ratio of 3 is the lowest limit for making monodisperse NPs.[6] Yang *et al.*[7] and Hyeon *et al.*[8] have reported that a ratio of OA/$Fe(acac)_3$ over 4 can produce Fe_3O_4 nanocubes, while Sun *et al.* prepared spherical Fe_3O_4 NPs using a similar method with the ratio of OA/$Fe(acac)_3$ less than 3.[9] Wu *et al.* have observed that the ratio of two surfactants can have a non-monotonic influence on the size of UO_2 NPs.[10] In order to achieve the gram-scale or kilogram-scale synthesis of NPs, it is greatly important to reveal a general law to control the size and size distribution in the scale-up synthesis of NPs based on an investigation on the influence of the stepwise increase of concentration and the ratio of the surfactants and precursors on particle size and its distribution.

In this paper, we report the unexpected observation of a non-monotonic size change of monodisperse Fe_3O_4 NPs with a diameter of 3–20 nm in the scale-up synthesis with a product mass from 0.03 to 1.0 g. The low-cost and non-toxic reactants, including FeO·OH and oleic acid, were used for the scale-up synthesis of Fe_3O_4 NPs *via* a facile high-temperature organic-phase method. It is interestingly observed that particle size does

[a]*Beijing National Laboratory for Condensed Matter Physics, Institute of Physics, Chinese Academy of Sciences, Beijing 100190, P. R. China. E-mail: zhcheng@iphy.ac.cn; htyang@iphy.ac.cn; Fax: +86-10-82649485; Tel: +86-10-82648083*

[b]*Universität Duisburg-Essen, Fakultät für Physik, Duisburg 147057, Germany*

[c]*Key Laboratory of Cryogenics, TIPC, Chinese Academy of Sciences, Beijing 100190, P. R. China*

† Electronic supplementary information (ESI) available. See DOI: 10.1039/c3nr33950e

not decrease monotonously with either an increase of the molar ratio of OA to FeO·OH, or the decrease of precursor concentration, which is very different from most of the reported results.[11–13] Moreover, the reaction process is investigated *via* the time-dependent FTIR spectra and TEM images, which reveal that OA has a different influence on the reaction stages with an increasing amount of precursor.

II Experimental

Nanoparticle synthesis

FeO·OH (50–80 mesh), 1-octadecene (ODC) and OA were purchased from Aldrich Chemical Co. All the other chemicals used in this work were of analytical reagent grade without the need for further purification. In a typical experiment for 5 nm NPs, 0.528 g (6 mmol) of FeO·OH, 10.296 g OA (36 mmol), and 40 mL of ODC were combined in a three-neck round-bottom reaction flask. The mixture was heated to 315 °C with a heating rate of 10 °C min^{-1} under magnetic stirring, and refluxed at this temperature for 1 h. The initial reddish-brown color of the reaction solution turned to brownish-black. The reaction solution was then cooled to room temperature by removing the heat source. Under air conditions, ethanol and acetone were added to the mixture, and a black material was separated *via* centrifugation. The black product was then dissolved in hexane. Centrifugation (3000 rpm) was applied to remove any aggregation residues. The product was then precipitated with ethanol, centrifuged (8000 rpm) to remove the solvent, excess surfactants and NPs with smaller sizes, and re-dispersed in hexane. After washing, the yield of Fe_3O_4 NPs was about 80%. In order to obtain the sample with a much narrower size distribution, the above separation procedure can be repeated several times; this is named as the size-selective treatment. After two size-selective treatments, the yield of Fe_3O_4 NPs decreased to about 70%.

Nanoparticle characterization

TEM was performed on a Toshiba H8100 at 120 kV and was used to determine particle shape and size distribution. Samples for TEM were prepared by drying the NP solutions on amorphous carbon-coated copper grids. High resolution TEM (HRTEM) showed the lattice structure of individual particles. XRD was used to characterize the crystal structure of the samples using step-scanning with a 0.02° step and 5 s integration time. Mössbauer spectroscopy was used to investigate the valence state of the Fe ions and the structure of the nanoparticles. The Mössbauer spectrum of ^{57}Fe at room temperature was recorded by a Wissel constant acceleration Mössbauer spectroscopy system with a ^{57}Co (Rh) source. The values of CS given here are relative to the room temperature value of α-Fe. Thermogravimetric-differential scanning calorimetry (TGA-DSC) measurements were carried out by a Shimadzu TGA-50 instrument in which the heating procedure followed the actual reaction conditions. FTIR spectra of the particles on KBr pellets were recorded on a Nicolet 750 FTIR spectrometer. DC magnetization measurements were performed on a Superconducting Quantum Design (SQUID) magnetometer (MPMS-XL). Zero-field-cooled (ZFC) and field-cooled (FC) DC magnetization measurements were carried out between room temperature and 20 K with a 100 Oe field. The measurements of the magnetization as a function of the magnetic field were carried out at 300 K in fields between −50 kOe and +50 kOe.

III Results and discussions

The TEM images of as-prepared 3, 5, 12, and 16 nm NPs without special size-selective treatment are shown in Fig. 1. The relative standard deviation of the size distribution is less than 10% and decreases to 5% after a size-selective treatment. The TEM images show that the NPs without special size-selective treatment can form partially ordered structures, rather than form superlattices in a big area. After size-selective treatment, the size distribution can be extremely narrowed, and the typical superlattices with a big area for the 3 nm and 16 nm samples are shown in Fig. 1e and f. The typical HRTEM images of the 12 nm NPs show that they are single crystalline, as indicated clearly by the atomic lattice fringes with the interfringe distance measured to be 0.292 nm for the (220) plane of the reversal spinel structure (the inset of Fig. 1c).

The XRD patterns of Fe_3O_4 NPs with particle sizes of 3 nm, 5 nm, 12 nm, and 16 nm, as shown in Fig. 2a, exhibit highly crystalline peaks that can be matched to the reverse spinel structure for pure bulk Fe_3O_4 (JCPDS no. 894319). Because magnetite and maghemite have very similar XRD patterns, we performed further characterizations by ^{57}Fe Mössbauer spectroscopy to distinguish the phases of iron oxide NPs (as shown in Fig. 2b). The Mössbauer spectra at room temperature were fitted using two magnetic components of hyperfine fields. The two sextets with hyperfine fields (H_{hf}), and the center shift (CS) of one (487.55 kOe and 0.32 mm s^{-1}) and the other (456.5 kOe and 0.66 mm s^{-1}) suggest the existence of Fe^{3+} and $Fe^{2.5+}$ ionic states. H_{hf} = 487.5 kOe and 456.5 kOe correspond to the Fe^{3+} ions on

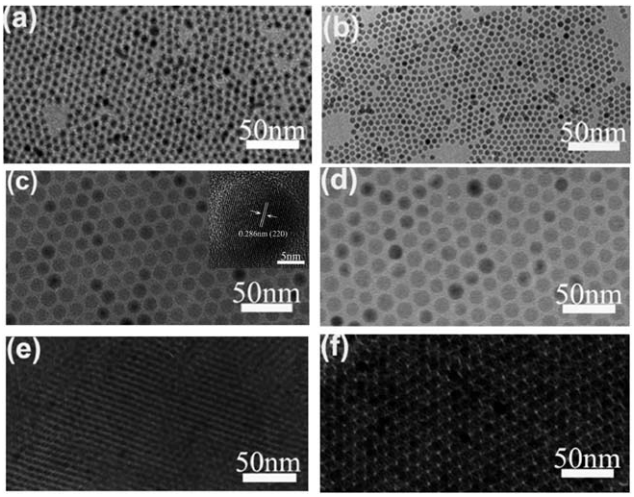

Fig. 1 TEM images of NPs with different sizes, (a) 3 nm, (b) 5 nm, (c) 12 nm, (d) 18 nm; TEM images with the large area-superlattices of samples with different sizes, (e) 3 nm, (f) 16 nm; an HRTEM image of the 12 nm sample is shown in the inset of figure (c).

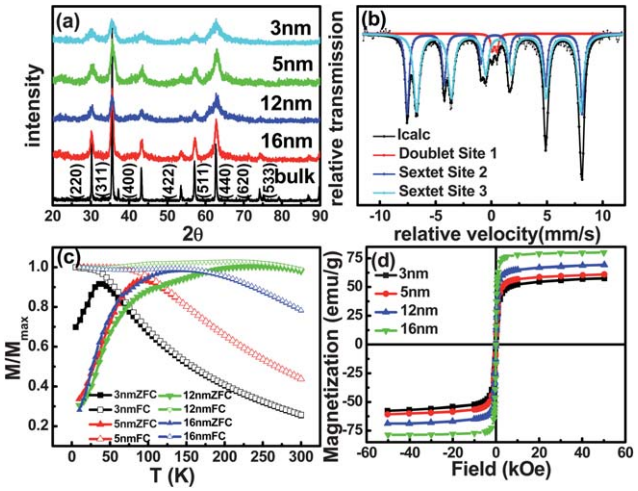

Fig. 2 (a) Powder XRD patterns of the NPs: 3 nm, 5 nm, 12 nm, 16 nm and bulk Fe_3O_4. (b) ^{57}Fe Mössbauer spectroscopy spectra for Fe_3O_4 NPs at room temperature. (c) ZFC (closed symbols) and FC (open symbols) magnetizations for the 3 nm, 5 nm, 12 nm and 16 nm samples. (d) Magnetic hysteresis loops at 300 K for the 3 nm, 5 nm, 12 nm and 16 nm samples.

the tetrahedral sites and the $Fe^{2.5+}$ (Fe^{2+} Fe^{3+}) ions on the octahedral sites, respectively. The results are consistent with the room-temperature results previously observed for magnetite NPs.[14,15] The two sextets were compared with a typical Mössbauer spectrum of bulk magnetite. The hyperfine field is lower than that of the bulk material and the resonance lines are broadened. The changes in the Mössbauer spectrum are due to the finite size effect, which can cause a higher percentage of surface atoms, additional stresses between atoms, and a superparamagnetic behavior.[16,17] Then the stoichiometry of the NPs was extracted by comparing the relative areas of $^{Tet}Fe^{3+}$ and $^{Oct}Fe^{2.5+}$ using the following equation $x = Fe^{2+}/Fe^{3+} = (1/2^{Oct}Fe^{2.5+})/(1/2^{Oct}Fe^{2.5+}+{}^{Tet}Fe^{3+})$.[18] The ratio of Fe^{2+} and Fe^{3+} is about 46.7%, which implies that the stoichiometry of the NPs is $Fe^{3+}{}_{2+0.066}Fe^{2+}{}_{1-0.066}O_4$. The possible reason for the slight shift of Fe^{3+} : $Fe^{2+} = 2$: 1 is the partial oxidation of Fe^{2+} ions on the surface layer or a slight presence of vacancies in the tetrahedral sites. The magnetic properties of Fe_3O_4 NPs with different sizes were studied. Fig. 2c shows the FC and ZFC obtained between 20 K and 300 K at an applied field of 100 Oe. All of the four samples show a superparamagnetic behavior. The blocking temperature, T_B, increases continuously as the diameter of the NPs increases, from 40 K, 96 K, 145 K to 235 K for the 3 nm, 5 nm, 12 nm, and 16 nm samples, respectively. The hysteresis loops of the Fe_3O_4 NPs with different sizes at 300 K are shown in Fig. 2d. The saturation magnetizations (M_s) at 300 K of the Fe_3O_4 NPs with sizes of 3, 5, 12, and 16 nm were 56.0, 59.0, 67.0 and 79.0 emu g^{-1}, respectively. The M_s value of the 16.0 nm Fe_3O_4 NPs is slightly lower than that of commercial magnetite powder (Alfa, Product no. 12962).

To reveal the varying law of particle size in the scale-up synthesis, we systematically investigated the influence of stepwise increasing the precursor concentration and the molar ratio of the surfactant-to-precursor, OA/FeO·OH, on the particle size from the microgram-scale to the gram-scale. A series of synthesis experiments was carried out with six different precursor concentrations, 0.0125 M, 0.05 M, 0.1 M, 0.15 M, 0.2 M, and 0.45 M, and different molar ratios of OA/FeO·OH, from 1 : 1 to 24 : 1. The influence of the reaction precursor and surfactant/precursor ratio on particle size is summarized in the table shown in the ESI.† Particle size as a function of the precursor concentration is plotted in Fig. 3a. It was found that at all four molar ratios of OA/FeO·OH the particle size has a non-monotonous change with an increasing concentration of precursor. When the ratio of OA/FeO·OH was 1 : 1 the size changed slightly from 20 nm to 18 nm by increasing the concentration from 0.0125 M to 0.2 M. When the ratio of OA/FeO·OH was 4 : 1, the size changed greatly from 20 nm to 2 nm and then to 18 nm by increasing the concentration from 0.0125 M to 0.1 M and 0.2 M, respectively. These results mean that the scale-up synthesis of Fe_3O_4 NPs with an expected size can not be achieved only by increasing the amount of all the reactants at the same equal proportion and that the size is greatly sensitive to the molar ratio of OA/FeO·OH. Therefore, the relationship between nanoparticle size and the ratio of OA/FeO·OH at different precursor concentrations was further investigated (as shown in Fig. 3b). With an increasing OA/FeO·OH ratio, the variation of particle size is not monotonous, decreasing at first, then increasing, and decreasing again at all concentrations. It should be noted that in the first decreasing stage and the subsequent increasing stage, the yield of NPs is not significantly changed with the increase of OA/FeO·OH. In the second decreasing stage, the yield of NPs decreases dramatically, and if the ratio is over a critical value no NPs precipitate from the reaction solution. In Fig. 3b, with increasing precursor molar amounts between 0.0125 M and 0.2 M, the critical OA molar ratios are 24, 13, 13, 10, and 10, respectively. This indicates that the extremely high OA amount does indeed suppress the formation of monomers and the subsequent nucleation. To reveal the scale-up synthesis law, a three dimension (3D) schematic diagram of the influence of the precursor concentration and reactants ratio on particle sizes is shown in Fig. 3c using interpolation calculation. Several laws for the gram-scale synthesis can be clearly concluded: (1) a larger ratio of surfactant/precursor has no remarkable effect on enlarging the adjusting scope of size and 10 is usually enough to obtain 1–50 nm NPs for cost-effectiveness; (2) below the ratio of 10, the adjusting scope for the same size shows a pyriform-ring shape, and with the precursor concentration increasing, the adjustable scope shrinks to the pear-neck-shaped part, which indicates that an extremely high precursor concentration is not beneficial for size control in the scale-up synthesis over the gram-scale; (3) in the scale-up synthesis, a high surfactant/precursor ratio is usually good for narrowing the size distribution and thus the surfactant/precursor ratio limited between 5 and 10 is an overall consideration of high-quality and cost-effectiveness.

In order to understand the thermal decomposition process of FeO·OH and determine the role of OA in the scale-up synthesis, we carried out a time-dependent FTIR analysis and TGA-DSC for three typical OA/FeO·OH molar ratios in series, 3 : 1, 6 : 1, and 9 : 1, with a 0.15 M precursor concentration. The

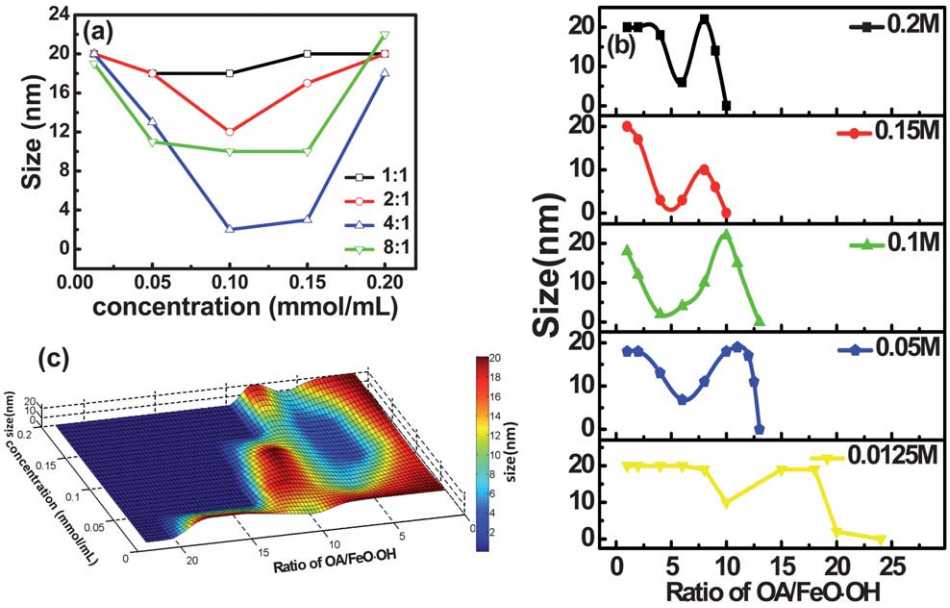

Fig. 3 (a) The relationship between the average size and precursor concentration with the ratio OA/FeO·OH 1 : 1 (□), 2 : 1 (○), 4 : 1 (△) and 8 : 1 (▽). (b) The relationship between the average size and the ratio OA/FeO·OH with the concentration 0.5 M (▼), 2 M (★), 4 M (▲), 6 M (●) and 8 M (■). (c) 3D schematic diagram of the influence of the precursor concentration and reactants ratio on particle size.

specimens for the time-dependent FTIR spectra were prepared by directly extracting hot aliquots (1 mL) of the reaction mixture (6 mmol FeO·OH, 40 mL ODC) at different reaction stages: dissolved (250 °C), refluxing point (315 °C), refluxing for 2 min, 5 min, 10 min, 30 min, 60 min, and 90 min (315 °C). The spectra of samples with the molar ratio of 3 : 1 are shown in Fig. 4a. Compared with the spectrum of OA, the obvious difference is that two peaks located at 1598 cm^{-1} and 1552 cm^{-1} appear after dissolving above 250 °C, which indicates the formation of an iron carboxylate complex. Generally, the characteristic peaks of iron-oleate are near 1608 cm^{-1}, 1519 cm^{-1} and 1444 cm^{-1}.[19] This reveals that an iron carboxylate complex, possibly (FeO)–COOR (R represents the carbon chain) and not iron oleate, formed above 250 °C by unidentate or bidentate coordination modes between Fe^{3+} and the –COOR group from the in-site reaction of FeO·OH and OA. The two peaks disappear after refluxing for 10 min, which indicates that the iron carboxylate complex, as the intermediate product, completely decomposes to iron oxide monomer by refluxing for a short time at 315 °C. However, for the OA/FeO·OH ratios of 6 : 1 and 9 : 1, only a broad peak appears at temperatures above 250 °C, possibly because the excess OA interacts with the COO–Fe group which leads to the shift of the characteristic peaks of the iron carboxylate complex to a combined broad peak. The combined broad peak disappears after 60 min in the case of the OA/FeO·OH molar ratio of 6 : 1, and still exists even after 90 min in the case of the OA/FeO·OH molar ratio of 9 : 1. This reveals that the iron carboxylate complex completely decomposes after 10 min, 30 min and more than 90 min when the solution reaches 315 °C for the ratios of OA/FeO·OH 3 : 1, 6 : 1 and 9 : 1, respectively. The peaks at 1708 cm^{-1} and 1463 cm^{-1} are the characteristic C=O and C–H (CH_2) groups on OA. The peaks at 1411 cm^{-1} and 1284 cm^{-1} can be associated with the C–O–H in-plane bend (δ_{C-O-H}) and the C–OH stretch (ν_{C-OH}).[20] During the reaction process the C–H (CH_2) group (1463 cm^{-1}) hardly changed, C–O–H (1411 cm^{-1}) and C–OH (1284 cm^{-1}) almost disappeared but the C=O (1708 cm^{-1}) peak slightly shifted to 1716 cm^{-1} and the relative peak intensity decreased (Fig. 4a). The C=O (1708 cm^{-1}) peak intensity shows an obvious decrease after refluxing at 315 °C for only 2 min, and a slow decrease in the case of the OA/FeO·OH molar ratios of 6 : 1 and 9 : 1 as shown in Fig. 4b and c. These

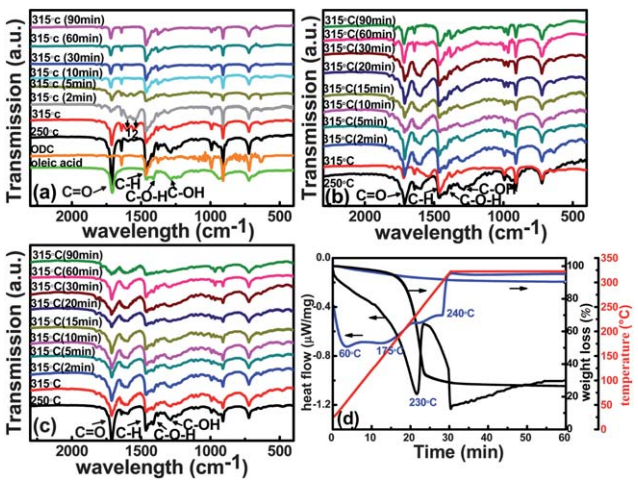

Fig. 4 The FT-IR spectra of the reaction solution (a) OA/FeO·OH is 3 : 1, FeO·OH is 6 mmol/40 mL aged at 250 °C (dissolved), 315 °C (refluxing), 315 °C for 5 min, 30 min and 1 h, respectively, (b) OA/FeO·OH is 6 : 1, FeO·OH is 6 mmol/40 mL aged at dissolved, refluxing moment, for 2 min, for 5 min, for 10 min, 15 min, 20 min, 30 min and 1 h, (c) OA/FeO·OH is 9 : 1, FeO·OH is 6 mmol/40 mL aged at dissolved, refluxing moment, for 2 min, for 5 min, for 10 min, 15 min, 20 min, 30 min and 1 h. (d) TGA and DSC profile of FeO·OH powder (blue) and sample with OA/FeO·OH 3 : 1 (black).

results clearly indicate that C=O (1708 cm^{-1}), C–O–H (1411 cm^{-1}) and C–OH (1284 cm^{-1}) played an important role in producing Fe_3O_4 NPs. The synthesis process can be concluded with some of the C=O groups (1708 cm^{-1}) on OA taking part in the synthesis of the iron carboxylate complex above 250 °C and some absorbing on the monomer and Fe_3O_4 nuclei as a surfactant so as to control the nucleation and growth of Fe_3O_4 NPs. In Fig. 4d, the TGA-DSC traces of the pure FeO·OH powder (Aldrich, product no. 371254) and the mixed OA/FeO·OH with the molar ratio of 3 : 1 are presented. The DSC trace of the pure FeO·OH powder shows three endothermic peaks at 60, 175, and 240 °C that can be assigned to the removal of absorbed water, the removal of crystal hydrate water, and the decomposition of FeO·OH, respectively. And during aging at 315 °C, the trace is nearly a horizontal line which indicates that no endothermic reaction happens. In the case of the mixed OA/FeO·OH, two obvious endothermic peaks at 230 and 315 °C are observed which can be assigned to the formation and subsequent decomposition of an iron carboxylate complex. During aging at 315 °C, the trace keeps slightly increasing for a long aging time. Such results reveal that most of the iron carboxylate complex decomposes within 10 min after the reaction temperature arrived at 315 °C, but there still exists a small amount of iron carboxylate complex decomposing in the subsequent aging process.

Based on these experimental results, a possible mechanism for the non-monotonic size change in the scale-up synthesis of Fe_3O_4 NPs is presented combined with some nucleation and growth theory. In our scale-up synthesis process, the reaction solution prepared at room temperature is heated to a high temperature to produce NPs, which is called the "heating-up" method. The "heating-up" method is quite different from the "hot injection" method in that there is no operation that induces high monomer supersaturation instantaneously. High monomer supersaturation induced by "hot injection" leads to a fast homogeneous nucleation reaction that is followed by a diffusion-controlled growth process, in which "focusing" of the particle size distribution occurs.[21] In the "heating-up" process, the generation of monomers occurs for a relatively long time and follows simultaneously the nucleation and growth of the NPs. Our synthesis process of Fe_3O_4 NPs is composed of three sequential steps. The first step is the formation of an iron carboxylate complex *in situ*, the second is the thermal decomposition of the iron carboxylate complex to form a monomer, and the third is the nucleation and growth of the Fe_3O_4 NPs. The thermal decomposition reaction of the transition iron carboxylates occurs *via* the formation of thermal free radicals. The break up of the Fe–O and FeO–C bonds of the iron carboxylate results in radical species as shown in eqn (1) and (2).[22,23]

$$\mathrm{Fe{-}OOCR} \rightarrow \mathrm{Fe^{\cdot}} + \mathrm{RCOO^{\cdot}} \quad (1)$$

$$\mathrm{Fe{-}OOCR} \rightarrow \mathrm{FeO^{\cdot}} + \mathrm{RC^{\cdot}O} \quad (2)$$

These radical species can recombine, decompose into smaller molecules, or react with other iron carboxylate molecules to propagate the decomposition reaction. Usually, the thermal decomposition of iron carboxylates in the solid state leads to the formation of iron oxide along with other byproducts such as CO, CO_2, H_2, water, ketones, esters, and hydrocarbons with various chain lengths. Although some reaction equations have been suggested for the thermal decomposition of iron carboxylates, the reaction route for the formation of iron oxide and the exact stoichiometric relations are not clear. A transparent solution was observed until 250 °C and no precipitate was found after an 8000 rpm centrifugation, which indicate that the powdery FeO·OH had dissolved as a kind of iron carboxylate complex from the reaction between FeO·OH and OA at this thermal condition. It was found that below 300 °C, there were no NPs produced. The formation of iron oxide NPs only takes place above 315 °C. After refluxing for 5 min, the typical peaks corresponding to the carboxylate group are still observed in the FTIR spectra and disappear after refluxing for 10 min, which indicates that such a "heating-up" method goes through a slow pyrolysis of the iron carboxylate complex. To trace the nucleation and growth process of Fe_3O_4 NPs, we obtained TEM images of a series of aliquots drawn from the reaction solution during the refluxing procedure (as shown in Fig. 5). In Fig. 5a the TEM image of the aliquot taken after refluxing at 315 °C for 2 min shows particles with a mean diameter of 3 nm and an irregular shape. In Fig. 5b both small NPs and big NPs with size up to 10 nm have been observed after refluxing for 5 min. With the reaction going on at 315 °C for 10 min the size becomes uniform around 10 nm and the shape regularly spherical. At the same time, the small nanoparticles almost disappear. Considering the time during which they reach a nearly fixed size, the small NPs seem to be at the stage just after nucleation in the homogeneous solution. If this is the case, from the size distribution data, it can be deduced

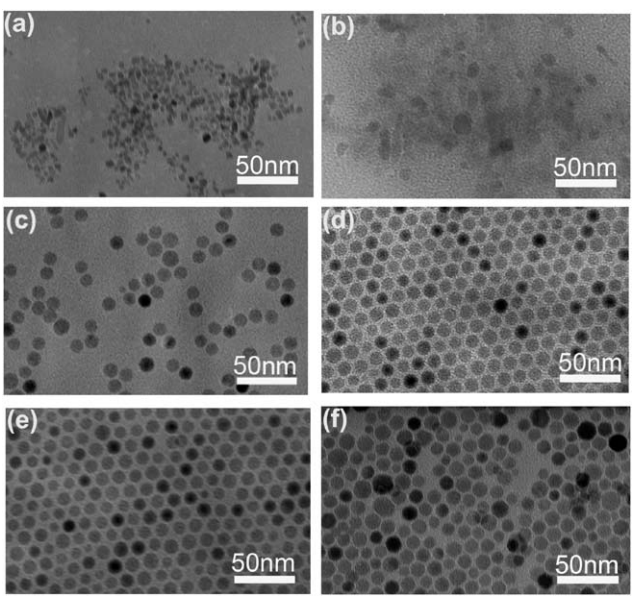

Fig. 5 TEM images of the samples (OA/FeO·OH is 3 : 1, FeO·OH is 6 mmol/40 mL) taken after refluxing at 315 °C for 2 min (a), 5 min (b), 10 min (c), 30 min (d), 60 min (e), 90 min (f).

that the nucleation process terminated after a 10 min aging at 315 °C in which the iron carboxylate complex also completely decomposes, as seen from the FTIR results. From Fig. 5a–c it is clear that the NPs grew quickly and that they aged at 315 °C. In the following aging, their surface became smoother and rounder, while their growth rate slowed down, as can be seen by comparing Fig. 5d and f after a 30 min and 60 min aging at 315 °C. After that, further aging of the NPs resulted in a broadening of the size distribution and the changing of the particle shape from spheres to an irregular shape after aging for 90 min, as shown in Fig. 5e. If the monomers can dissolve and reprecipitate on the crystal surface reversibly in the solution, they will have a tendency to migrate from a higher to a lower free energy region. When the monomer concentration is low, this tendency leads to the ripening process in which the intra- and inter-particle redistribution of the monomers occurs. Through this process, the morphology of the NPs changes to a thermodynamically stable one with a smooth surface. Because smaller particles have higher surface free energy due to the Gibbs–Thomson effect, the monomers moved from smaller to larger particles. Thus, in addition to the morphology change, the broadening of the size distribution also occurs by the ripening process. The inter-particle redistribution of the monomers is well known as Ostwald ripening.

Now a clear understanding of the "heating up" synthesis process is present, which goes through a slow monomer formation period *via* the pyrolysis of the iron carboxylate complex, a slow and continuous nucleation, and a fast growth stage *via* Ostwald ripening. Combined with the nucleation–growth theory for NPs and further experiments, we expect to give a reasonable explanation on the observed behavior of the non-monotonic size change in our scale-up synthesis. From the FTIR results, with the molar ratio of OA/FeO·OH less than 5 : 1, the carboxylate group at all precursor concentrations except 0.0125 M disappears after aging at 315 °C for 10 min. With an increasing molar ratio of OA/FeO·OH between 5 : 1 and 10 : 1, the carboxylate group disappears after aging at 315 °C for 60 min. For a high molar ratio of OA/FeO·OH over 10 : 1, the carboxylate group does not disappear even after aging for 90 min and nearly no NPs can be observed. So we deduce that OA has an influence on (1) the growth stage below the molar ratio of OA/FeO·OH of 5 : 1, (2) the nucleation stage between the molar ratio of OA/FeO·OH of 5 : 1 and that of 10 : 1, (3) the monomer formation stage above the molar ratio of OA/FeO·OH of 10 : 1. For the extremely low precursor concentration of 0.0125 M, the molar ratio of OA/FeO·OH can extend to 10 : 1 and 18 : 1 as partition points. For the molar ratio of OA/FeO·OH less than 5 : 1 or 10 : 1 in the extremely low precursor concentration case, the remaining amount of OA after consumption in the formation of iron carboxylate is not enough to dissolve the monomers or prevent the progress of the pyrolysis of the iron carboxylate, and only plays a role in preventing the growth of NPs *via* Ostwald ripening, which results in a decreasing particle size with an increasing ratio of OA/FeO·OH. Over the critical value of 5 : 1 or 10 : 1 in the extremely low precursor concentration case, the remaining OA after consumption in the formation of the iron carboxylate can have an ability to dissolve the monomers, or an exacter explanation would be that the dissolving speed of the monomers is more than that of reprecipitation on the particle surface, which results in a decrement of the amount of nucleation and more monomers are thermodynamically driven to grow on the small NPs leading to an increment of NP size. By increasing the ratio of OA/FeO·OH over another critical value, 10 : 1 or 18 : 1, in the extremely low precursor concentration case, the remaining OA has a high enough chemical potential to suppress the progress of the pyrolysis of the iron carboxylate, which results in a dramatic decrease of both the monomers and the nuclei leading to small particle size and low yield of NPs.

Though our present mechanistic studies are qualitative or empirical, we expect to provide some revelatory information for other researchers from such a rapid report. We shall next build a theoretical model to describe the "heating-up" process according to the Finke–Watzky[24] two-step kinetic mechanism consisting of (a) a slow, continuous nucleation and then (b) a fast, autocatalytic surface growth, and perform a numerical simulation based on this model. Through further theoretical models, the mechanism underlying the control of the size and size distribution in the "heating-up" method can develop a general technical route for the gram- or kilogram-scale synthesis of uniform-sized NPs.

IV Conclusions

We have presented a scale-up synthesis of Fe_3O_4 NPs from 3 to 20 nm by changing the concentration of the precursor and the ratio of the surfactant/precursor in a wide range using a facile organic-phase synthesis method. Under a six stepwise increase in the concentration of precursor, the size of the Fe_3O_4 NPs did not show a monotonic change with an increasing molar ratio of OA/FeO·OH. The surfactant played different roles, including preventing the aggregation of small NPs, suppressing the nucleation process, and inhibiting the pyrolysis of the iron carboxylate, in controlling the size of Fe_3O_4 NPs in different stages of the "heating-up" synthesis method. Since the "heating-up" method which is simple, economical, flexible, and safe, is propitious to applications in the industrial production of monodisperse Fe_3O_4 nanoparticles, it is expected that such a non-monotonic change of particle size in scale-up synthesis is helpful not only for the further understanding of nucleation and growth processes in the "heating-up" method, but also for the development of the gram-scale or kilogram-scale synthesis technique of monodisperse NPs.

Acknowledgements

We gratefully thank Prof. S. H. Sun and Prof. C. M. Shen for their helpful discussions and suggestions. This work was supported by the National Basic Research Program of China (Grant no. 2012CB933102, 2011CB921801 and 2010CB934202) and the National Natural Sciences Foundation of China (51071173, 11274370, and 50931006).

References

1 L. Brannon-Peppas and J. O. Blanchette, *Adv. Drug Delivery Rev.*, 2004, **56**, 1649.
2 T. Osaka, T. Matsunaga, T. Nakanishi, A. Arakaki, D. Niwa and H. Iida, *Anal. Bioanal. Chem.*, 2006, **384**, 593.
3 H. Gu, K. Xu, C. Xu and B. Xu, *Chem. Commun.*, 2006, 941.
4 E. J. W. Verwey, *Nature*, 1939, **144**, 327.
5 S. G. Kwon, Y. Z. Piao, J. N. Park, S. Angappane, Y. H. Jo, N. M. Hwang, J. G. Park and T. Hyeon, *J. Am. Chem. Soc.*, 2007, **129**, 12571.
6 X. W. Teng and H. Yang, *J. Mater. Chem.*, 2004, **14**, 774.
7 H. T. Yang, T. Ogawa, D. Hasegawa and M. Takahashi, *J. Appl. Phys.*, 2008, **103**, 07D526.
8 D. Kim, N. Lee, M. Park, B. H. Kim, K. J. An and T. Hyeon, *J. Am. Chem. Soc.*, 2009, **131**, 454.
9 S. Sun and H. Zeng, *J. Am. Chem. Soc.*, 2002, **124**, 8204.
10 H. M. Wu, Y. A. Yang and Y. C. Cao, *J. Am. Chem. Soc.*, 2006, **128**, 16522.
11 Y. W. William, J. C. Falkner, C. T. Yavuz and V. L. Colvin, *Chem. Commun.*, 2004, 2306.
12 R. Vijayakumar, Y. Koltypin, I. Felner and A. Z. Gedanken, *Mater. Sci. Eng., A*, 2000, **286**, 101.
13 J. Park, K. An, Y. Hwang, J. Park, H. Noh, J. Kim, J. Park, N. Hwang and T. Hyeon, *Nat. Mater.*, 2004, **3**, 891.
14 E. Lima, Jr, E. D. Biasi, M. V. Mansilla, M. E. Saleta, F. Effenberg, L. M. Rossi, R. Cohen, H. R. Rechenberg and R. D. Zysler, *J. Appl. Phys.*, 2010, **108**, 103919.
15 K. Woo, J. Hong, S. Choi, H. W. Lee, J. P. Ahn, C. S. Kim and S. W. Lee, *Chem. Mater.*, 2004, **16**, 2814.
16 R. M. Cornell and U. Schwertmann, *The Iron Oxides*, Wiley-VCH, Weinheim, Germany, 2003.
17 C. A. Gorski and M. M. Scherer, *Am. Mineral.*, 2010, **95**, 1017.
18 G. M. da Costa, E. de Grave, L. H. Bowen, P. M. A. de Bakker and R. E. Vandenberghe, *Clays Clay Miner.*, 1995, **43**, 562.
19 L. M. Bronstein, H. Xinlei, R. John, S. Abrin, P. Maren, S. D. Barry and D. Bogdan, *Chem. Mater.*, 2007, **19**, 3624.
20 P. J. Thistlethwaite and M. S. Hook, *Langmuir*, 2000, **16**, 4993.
21 X. Peng, L. Manna, W. Yang, J. Wickham, E. Scher, A. Kadavanich and P. A. Alivisatos, *Nature*, 2000, **404**, 59.
22 F. Kenfack and H. Langbein, *Thermochim. Acta*, 2005, **426**, 61.
23 A. S. Rozenberg and V. R. Stepanov, *Russ. Chem. Bull.*, 1996, **45**, 1336.
24 M. A. Watzky and R. G. Finke, *J. Am. Chem. Soc.*, 1997, **119**, 10382.